

Using Predictive Techniques within CNC Machine Tools Feed Drives

Mara Susanu, *Student Member IEEE*, and Didier Dumur

Abstract—The paper presents a hierarchical predictive control architecture dedicated to axis feed drives of machining centres. The primary level is built with Generalized Predictive Control (GPC) strategy, without considering any constraints action. The controller is formulated under the polynomial RST form, as a convenient framework for CNC systems. Robustification of this controller towards measurement noises that often drastically affect machine-tool environment is also examined. This basic level is further enhanced with a predictive-based mechanism allowing constraints avoidance by an adequate local change of the tool path. Finally, if this is action is not sufficient, as the full path during machining is known, an advanced constraints avoidance option is added, that may recompute the whole remaining trajectory with a lower speed profile. This strategy is validated in a virtual machining centre.

I. INTRODUCTION

Within the machining area, performances are formulated in terms of machining speed and accuracy.

Nowadays, high speed machining (HSM) as well as precision at micron level requires more complex control laws for the axis controllers [8]. The fulfillment of the imposed specifications implies on the one hand the use of more reliable actuators for the axis control, on the other hand the use of control laws known as “advanced laws”, allowing the optimization of the system behavior (stability, speed, precision and robustness). However, if changing the actuator proved to be rather easy, the control law on the CNC is generally completely closed. The virtual simulation environments are the only realistic solution to compare and analyze advanced control modules performances [13].

An indicator of accuracy in such systems is the contour error [6] – “the orthogonal deviation from the desired toolpath”. One of its main causes is the axial tracking error especially when machining at high speeds, as well as the disturbances (different types of friction and measurement noises). Starting from these requirements for axis control, the paper presents the construction of a hierarchical structure, with model-based predictive features basically formulated as in [11] by the knowledge of the trajectory to be followed at least for a certain horizon, the use of a process model, the control law resulting from an optimization of the predicted performance, the application of the receding horizon principle.

The first design step considers Generalized Predictive

Control (GPC) law for the basic level of feed drive positioning control, robustified against measurement noises and parameters uncertainty, implemented under the polynomial RST form. This advanced structure is designed without considering eventual constraints.

Further, saturations are considered through an upper model-based predictive level, with the entire controlled closed loop as new model. Using the known future trajectory, past control actions and past system outputs, the procedure computes the best admissible reference signal, over a certain prediction horizon, which avoids signal saturation, following the so-called “reference governor” term used in the literature [4].

Thus, incorporating two predictive-based techniques, the proposed architecture utilizes the complete tool path knowledge in order to improve the tracking accuracy and to avoid constraints saturation as well. These techniques, although based on the same philosophy, are completely independent. Therefore, modular structures might be derived in order to fit the open architecture demands [10] of most interest nowadays within the machining area.

Finally, taking into account the specificity that the trajectory to be followed is entirely known, and if the microprocessors within the CNC are powerful enough for on-line trajectory re-generation, an optional decisional level might be used if the other levels action is not sufficient for tracking accuracy requirements, which performs the re-parameterization of the tool path with a lower velocity profile.

The paper is organized as follows. The second section presents the robust feed drive control structure with a brief recall of the GPC main aspects. Section III introduces the predictive approach for constraints saturation avoidance, and a machining oriented approach for time re-parameterisation of the tool path. Section IV shows results obtained with a virtual machine-tool and conclusions are in Section V.

II. FEED DRIVE PREDICTIVE CONTROL

A. Predictive Control Orientation

Standard feed drive servo control structures include three cascaded position, velocity and current loops. These feedback controllers are very often of P type for position and PI(D) for velocity and current control. Feedforward controllers are added in order to decrease the tracking errors [7].

Based on this configuration, the proposed structure includes GPC laws for the position and velocity control. A GPC/MRM (Generalized Predictive Control with Multiple Reference Models) version is introduced in the inner velocity loop, whereas GPC version is considered in the

M. Susanu is with Supélec, Automatic Control Department, 91192 Gif-sur Yvette cedex, France (phone: +33 (0)1 69 85 13 84; fax: +33 (0)1 69 85 13 89; email: mara.susanu@supelec.fr).

D. Dumur is with Supélec, 91192 Gif-sur Yvette cedex, France (email: didier.dumur@supelec.fr).

external position loop. Details for this implementation can be found in [3]. The main steps for designing a GPC controller as given in [5] are summarized below.

The model of the process is given under the CARIMA (Controlled AutoRegressive Moving Average) form:

$$A(q^{-1})y(t) = B(q^{-1})u(t-1) + \xi(t)/\Delta(q^{-1}) \quad (1)$$

with $u(t), y(t)$ the process input and output, $\xi(t)$ a centered Gaussian white noise. The use of the operator $\Delta(q^{-1}) = 1 - q^{-1}$ ensures an integral control law or a closed loop type I system, A and B are polynomials in the backward shift operator q^{-1} , of respective degree n_a and n_b .

The predicted behavior of the system output (the optimal j -step ahead predictor noted \hat{y}), based on the previous model, is split in two components noted the ‘‘free response’’ and the ‘‘forced response’’. The first term corresponds to the past system outputs and past control actions, whereas the second term contains the future control actions, as follows:

$$\hat{y}(t+j) = \underbrace{F_j(q^{-1})y(t) + H_j(q^{-1})\Delta u(t-1)}_{\text{free response}} + \underbrace{G_j(q^{-1})\Delta u(t+j-1)}_{\text{forced response}} \quad (2)$$

where the F_j, G_j, H_j polynomials are solutions of:

$$\begin{aligned} \Delta(q^{-1})A(q^{-1})J_j(q^{-1}) + q^{-j}F_j(q^{-1}) &= 1 \\ G_j(q^{-1}) + q^{-j}H_j(q^{-1}) &= B(q^{-1})J_j(q^{-1}) \end{aligned} \quad (3)$$

The considered performance index is a weighted sum of predicted tracking errors from a minimum prediction horizon N_1 to a maximum horizon N_2 and future control signal increments over the control horizon N_u :

$$J = \sum_{j=N_1}^{N_2} [w(t+j) - \hat{y}(t+j)]^2 + \lambda \sum_{j=1}^{N_u} \Delta u(t+j-1)^2 \quad (4)$$

with λ a control weighting factor, w the setpoint and assuming that there will be no control changes after N_u steps, $\Delta u(t+j) = 0$ for $j \geq N_u$. The control law is derived through analytical minimization of Eq.4 and may be structured under the RST equivalent polynomial controller, simply implemented by a finite differences equation:

$$S(q^{-1})u(t) = -R(q^{-1})x(t) + T(q^{-1})x^*(t) \quad (5)$$

The controllers for both loops in Fig.1 are synthesized under this numerical framework, very attractive within CNC environment. The block ‘Feed drive model’ in Fig.1 corresponds to the inner PI current loops and the mechanical part [1]. The tuning parameters N_1, N_2, N_u, λ are usually chosen according to stability and robustness requirements [3] through a study of the open controlled loop.

The implementation of this type of control law for feed drives of machine tools provides a certain number of advantages. The main improvement compared to classical

strategies comes from the non causal T polynomial, generating a closed loop anticipative effect, so that difficult to tune open loop feedforward is not necessary anymore. Then, the two-degree of freedom strategy allows separation of the disturbance rejection and tracking capabilities [9]. Finally, the polynomial controllers are computed off-line, reducing the computational load so that the on-line part only results in the computation of simple differences equations Eq. 5. The controller polynomials are in most cases of small degrees, again reducing the computation time. This aspect allows the implementation of this strategy even with short sampling times (e.g. in the case of high speed machining).

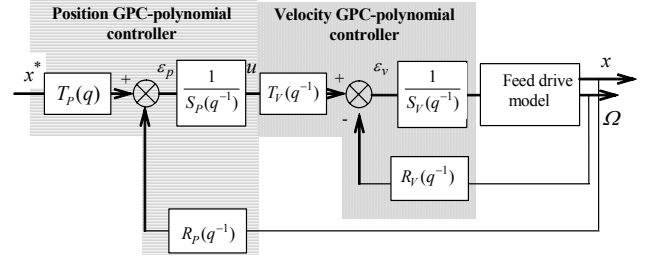


Fig. 1. RST GPC cascaded control for feed drive.

B. Robust predictive control

Predictive RST control laws as presented before may significantly improve performances in terms of accuracy. However, in the machine tool context, disturbances due to measurement noise or neglected dynamics within the model might affect the control actions in a significant way, justifying robustification of the controllers towards these uncertainties. Trying to remain within the same RST context for open architecture purposes, a methodology which is able to robustify any RST-type controller has been implemented, which also results in a RST-type robustified structure.

The procedure starts as first step with the design of an initial RST controller (of any type, e.g. either PID or GPC). Then the robustness of this initial controller towards model uncertainties or measurement noise is increased using the Youla parameter $Q(q^{-1})$. This parameterization allows formulating frequency and time-domain constraints as convex optimizations. Afterwards, this optimization problem is approximated by a linear programming with inequality constraints, and the optimal parameter belonging to the research set is derived. As main advantage, this parameter enables to find the set of all controllers stabilizing the system, structured under the form:

$$\begin{aligned} \tilde{T}(q^{-1}) &= T(q^{-1})(1 - Q_2(q^{-1})) \\ \tilde{R}(q^{-1}) &= R(q^{-1}) + \Delta(q^{-1})A(q^{-1})Q_1(q^{-1}) \\ \tilde{S}(q^{-1}) &= S(q^{-1}) - q^{-1}B(q^{-1})Q_1(q^{-1}) \end{aligned} \quad (6)$$

where $Q = [Q_2 \ Q_1]$ such that $Q_1(q^{-1}), Q_2(q^{-1})$ are stable transfer functions. As stated in Fig. 2, $Q_2(q^{-1})$ only affects the input/output behavior, and $Q_1(q^{-1})$ modifies the disturbance rejection behavior. Within the feed drive control module, $Q_2(q^{-1})$ is set to 0 as the required input/output behavior is assumed to be reached by the initial controller.

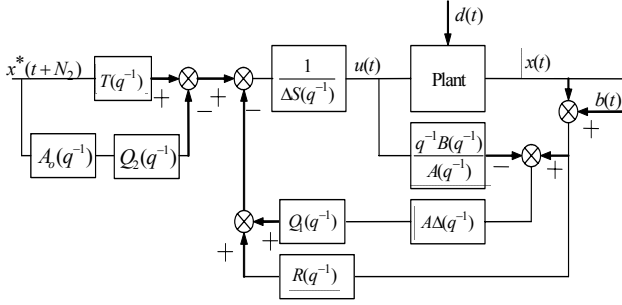


Fig. 2. Robustified RST structure.

Further the parameter $Q_1(q^{-1})$ results from an optimization problem taking into account frequencies for which the model has more uncertainties (weighted H_∞ norm in Eq. 7), measurement noise influence as a particular template ($\Phi_{env2}(Q_1)$ in Eq. 7), and time domain specifications, such as disturbance rejection dynamics, in terms of step response of the transfer disturbance-output (denoted $\Phi_{env1}(Q_1)$ in Eq. 7).

$$\min_{\substack{Q_1 \in \mathcal{RH}_\infty \\ \Phi_{env1}(Q_1) < 0, \Phi_{env2}(Q_1) < 0}} \left\| \left(-\frac{q^{-1}BR}{A_o A_c} - \frac{q^{-1}B\Delta A}{A_o A_c} Q_1 \right) W(q^{-1}) \right\|_\infty \quad (7)$$

where W is a weighting function and $A_o A_c = \Delta AS + q^{-1}BR$ the characteristic closed loop polynomial.

The new robust $\tilde{R} - \tilde{S} - \tilde{T}$ controller in this way has the same polynomial formulation as the initial one, its complexity is very slightly increased. Full developments of the method are given in [12].

III. USING PREDICTIVE CAPABILITIES FOR CONSTRAINTS AVOIDANCE

A. The Reference Supervisor

The predictive philosophy and the tool path knowledge can be employed for another kind of control problems as well. Starting from the predictive mechanism proposed in [2, 4], a “reference supervisor” which modifies the reference signal to avoid constraints saturation is now implemented as an additional module, at a superior level (see Fig. 3) on each axis control module. It can be designed for any linear time invariant controller under the RST form.

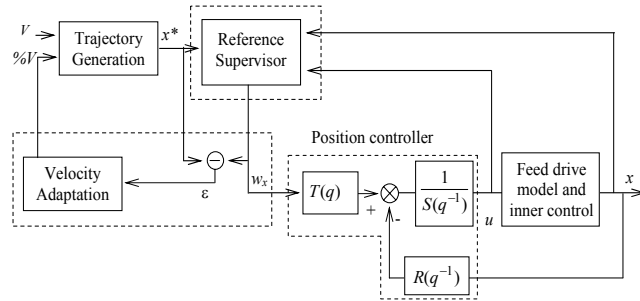


Fig. 3. Complete predictive control structure for one feed drive.

This block operates only if the control signal overcomes the constraints, otherwise it outputs the reference sequence unchanged as it was received from the machining centre

trajectory generation module (noted x^* in the figure).

Based on the receding horizon principle, and using the known future trajectory, the past control actions and output, the procedure computes the reference signal over a certain trajectory prediction horizon that avoids saturation of the control signals. In Fig. 3, for one axis control structure, the block “Feed drive model and inner control” hides the rest of the control structure as described earlier. The “Velocity Adaptation” function will be described further. The mathematical formulation given here is based on the RST structure and corresponds to constraints imposed on the control signal of the position loop, meaning the axial velocity setpoint (the same procedure can be developed in the inner loop for actuator constraints). Considering a convex quadratic optimization problem [4], the reference supervisor output w_m is computed at each sampling period from:

$$\mathbf{w}_m(t) = \arg \min_{\mathbf{w}_t} \left\| \mathbf{w}_t(t) - \mathbf{x}^*(t) \right\|_\Lambda^2 \quad (8)$$

under the constraints formulation described below, with $\Lambda = \Lambda^T > 0$ a weighting matrix, \mathbf{x}^* the initial reference sequence and $\|\mathbf{a}\|_\Lambda^2 := \mathbf{a}^T \Lambda \mathbf{a}$. This eventually modified reference is applied on the main controlled system input.

Generally, the limits on the control signal over the time horizon N_c can be written as:

$$\underline{\mathbf{U}} \leq [u(t) \dots u(t+N_c)]^T \leq \bar{\mathbf{U}} \quad (9)$$

with $\underline{\mathbf{U}} = [\underline{u}_1 \dots \underline{u}_{N_c}]^T$, $\bar{\mathbf{U}} = [\bar{u}_1 \dots \bar{u}_{N_c}]^T$ the lower and upper control signal limits. The control signal Eq. 5 is given in a matrix form by:

$$u(t) = [-\tilde{S} \quad -R \quad T] [\mathbf{u}_p(t) \quad \mathbf{x}_p(t) \quad \mathbf{w}_t(t)]^T \quad (10)$$

$$\begin{aligned} \text{with: } \mathbf{u}_p(t) &= [u(t-1) \dots u(t-n_S)]^T, \quad n_S = \deg(S), \quad S = 1 + \tilde{S} \\ \mathbf{x}_p(t) &= [x(t) \dots x(t-n_R)]^T, \quad n_R = \deg(R) \\ \mathbf{w}_t(t) &= [w_x(t+1) \dots w_x(t+n_T)]^T, \quad n_T = \deg(T) = N_2 \end{aligned}$$

For further formulations taking into account the trajectory prediction horizon, \mathbf{w}_t will be augmented to:

$$\mathbf{w}_t(t) = [w_x(t+1) \dots w_x(t+n_T+N_c-1)]^T \quad (11)$$

For the sake of computation with the non-causal T polynomial, the following evolution of \mathbf{w}_t is chosen:

$$\mathbf{w}_t(t+k) = [w_x(t+k+1) \dots w_x(t+k+n_T) \dots \dots w_x(t+n_T+N_c-1) \underbrace{0 \dots 0}_k], \quad k < N_c \quad (12)$$

Eq. 10 now becomes:

$$u(t) = \boldsymbol{\varphi} \boldsymbol{\theta}(t) \quad (13)$$

$$\text{with: } \boldsymbol{\theta}(t) = [\mathbf{u}_p(t) \quad \mathbf{x}_p(t) \quad \mathbf{w}_t(t)]^T \quad (14)$$

$$\boldsymbol{\varphi} = [-\tilde{S} \quad -R \quad \hat{T}]_{1 \times (n_S + n_R + n_T + N_c)}, \quad \hat{T} = \begin{bmatrix} T & \underbrace{0 \dots 0}_{N_c-1} \end{bmatrix} \quad (15)$$

Using Eqs. 10 and 13, and the system model Eq. 1, the evolution of $\theta(t)$ can further be expressed as:

$$\theta(t+k) = \Psi \theta(t+k-1) \quad (16)$$

$$\Psi = \begin{bmatrix} \begin{array}{c|c|c} -\tilde{S} & -R & \tilde{T} \\ \hline 1 & 0 & \dots & 0 \\ 0 & 1 & \dots & 0 & 0 & \dots & 0 & \vdots & \ddots & \vdots & \vdots & \ddots & \vdots \\ \vdots & \vdots & \ddots & \vdots \\ 0 & 0 & \dots & 1 & 0 & \dots & 0 & 0 & \dots & 0 & 0 & \dots & 0 \end{array} & \begin{array}{c|c|c} -b_0 \tilde{S} + \hat{B} & -b_0 R - [\tilde{A} \ 0] & b_0 \hat{T} \\ \hline 0 & 1 & 0 & 0 & 0 & 0 & 0 & 0 & \dots & 0 & 0 & \dots & 0 \\ \vdots & \vdots & \vdots & 0 & 1 & \dots & 0 & 0 & \vdots & \vdots & \vdots & \ddots & \vdots \\ \vdots & \vdots & \vdots & \vdots & \vdots & \ddots & \vdots & \vdots & \vdots & \vdots & \vdots & \ddots & \vdots \\ 0 & 0 & \dots & 0 & 0 & 0 & \dots & 1 & 0 & 0 & \dots & 0 & 0 \end{array} \\ \hline \begin{array}{c|c|c} 0 & 0 & \dots & 0 & 0 & \dots & 0 & 0 & 1 & 0 & \dots & 0 & 0 \\ \vdots & \vdots & \ddots & \vdots & \vdots & \ddots & \vdots & \vdots & \vdots & \vdots & \vdots & \ddots & \vdots \\ \vdots & \vdots & \vdots & \vdots & \vdots & \ddots & \vdots & \vdots & \vdots & \vdots & \vdots & \ddots & \vdots \\ 0 & 0 & \dots & 0 & 0 & \dots & 0 & 0 & 0 & 1 & \dots & 0 & 0 \end{array} & \begin{array}{c|c|c} 0 & 0 & \dots & 0 & 0 & \dots & 0 & 0 & 0 & 0 & \dots & 0 & 0 \\ \vdots & \vdots & \ddots & \vdots & \vdots & \ddots & \vdots & \vdots & \vdots & \vdots & \vdots & \ddots & \vdots \\ \vdots & \vdots & \vdots & \vdots & \vdots & \ddots & \vdots & \vdots & \vdots & \vdots & \vdots & \ddots & \vdots \\ 0 & 0 & \dots & 0 & 0 & \dots & 0 & 0 & 0 & 0 & \dots & 1 & 0 \end{array} \end{bmatrix} \quad (17)$$

where: $A = 1 + \tilde{A}$, $B = [b_0 \ \hat{B}]$ (18)

Considering the previous notations and Eq. 9 leads to:

$$\underline{U} \leq \underbrace{\begin{bmatrix} \hat{\Sigma} \\ \underline{\Sigma} \end{bmatrix}}_{\Sigma^*} \begin{bmatrix} \mathbf{u}_p(t) \\ \mathbf{y}_p(t) \\ \mathbf{w}_t(t) \end{bmatrix} \leq \overline{U}, \quad \Sigma^* = \begin{bmatrix} \phi & \phi & \Psi & \dots & \phi & \Psi^{N_c} \end{bmatrix}^T \quad (19)$$

The multiparametric inequality has to be considered for the selection of the modified trajectory N_c -steps ahead in a convex constrained quadratic optimization problem Eq. 8:

$$\begin{bmatrix} -\underline{\Sigma} \\ \overline{\Sigma} \end{bmatrix} \mathbf{w}_t(t) \leq \frac{\begin{bmatrix} \underline{U} + \hat{\Sigma} \\ \overline{U} + \hat{\Sigma} \end{bmatrix} \begin{bmatrix} \mathbf{u}_p(t) \\ \mathbf{y}_p(t) \\ \mathbf{u}_p(t) \\ \mathbf{y}_p(t) \end{bmatrix}}{\quad} \quad (20)$$

The initial reference, modified only in case of constraints saturation leading to wind-up effects and deterioration of the closed loop performance, is applied to the main controlled system input and the procedure is repeated at each sampling period, following the receding horizon principle. However, the module may work at a slower sampling rate than the GPC controllers to decrease the computational load.

It is clear that this modified setpoint will affect the tracking performances but to a lesser extent than with wind-up effect (even with GPC implementation taking into account saturated control values). Fig. 4 gives an example for a one axis movement of 100mm, performed at 60mm/s linear velocity. In fact, considering the machining area, no trajectory constraints overcome should appear since axial velocities are directly handled during the design phase. But, while machining, changes within the cutting forces profile for example might cause torque disturbances and thus the limits of the velocity setpoint might be surpassed. In order to simulate these actions, white noise acting at the torque level has been introduced within the model. Therefore, one may

see from Fig. 4b) that the unconstrained velocity setpoint is forced to overcome the limit, supposed to be here at 60mm/s. Amelioration achieved with the reference supervisor is obvious in Fig. 4a) with a decrease of the tracking errors ($x^* - x$) in transient. The predictive action might be noticed in the transitory part of the velocity Fig. 4b). The example presented had no hard constraint imposed. In case of saturation with wind-up, improvement is even more obvious.

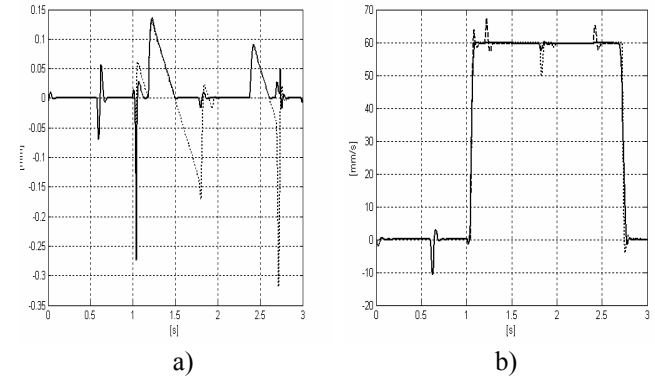


Fig. 4. Supervisor action – solid, saturation – dotted. a) tracking error. b) velocity setpoint (unconstrained case - dashed).

B. A link with the trajectory generation task

As explained before, the reference supervisor action involves the trajectory modification in order to avoid the saturation. Changing the trajectory improves the error compared to the classical saturation effects, but the degradation remains. Within the machining area, as the goal is to obtain a contour error as small as possible for a machining speed as high as possible, advantages can be further obtained from the trajectory generation tasks, if the interpolation is performed rather rapidly.

During the trajectory generation, a simple toolpath is sent in segments to the interpolator; then, imposing a certain velocity profile and an interpolation algorithm, the reference points for each individual axis are elaborated, as well as the axial velocities profiles. Starting from these ideas, the principle proposed in the paper is simple: once the trajectory predicted by the reference supervisor is too strongly modified, the velocity adaptation might come into action. This is illustrated in Fig. 3, adding the block “velocity adaptation” by the error ε , between the modified reference, w_t and x^* . As the same trajectory can be covered with a lower velocity in a longer time, this module brings a compromise between the machining time and the tracking error by managing the velocity for the displacement along the desired trajectory. The known remaining trajectory might be reparameterised considering a lower velocity for the imposed profile. The axial reference points are then recomputed, starting from a specific point in the future, in order to insure parallel actions: the machining is not interrupted while the trajectory is recomputed.

C. Computational aspects

A complex problem for the presented structure is the choice of the different tuning parameters linked also to the

computational load. A review of the main characteristics is formulated in table 1.

TABLE I
SOME FEATURES OF THE PROPOSED STRUCTURE

Levels	Model based	Receding horizon	Prediction horizons min-max	Influence	Applied values
GPC	✓	✓	$N_1 - N_2$	control law	1
RS	✓	✓	N_c	setpoint	N_2
VA	X	X	$P_{future} - P_{final}$	toolpath	all

As shown in previous sections, both feed drives controllers and reference supervisor are model-based predictive modules. The prediction horizons for the GPC law are N_1 and N_2 as defined earlier, linked to the delay and response time of the process, chosen to provide specified input/output behavior. Concerning the reference supervisor, the value of the trajectory prediction horizon N_c might be computed off-line (see algorithm in [2]). Conversely, experiences prove that a too large prediction horizon might not bring significant changes in improving performances. According to the computing capabilities of the CNC, the RS task might act at a reduced sampling time.

The GPC law is computed over the N_2 horizon and from this sequence, only the first value is applied according to the receding horizon principle. Concerning the reference supervisor, from the $N_c + N_2 - 1$ computed predicted references, only N_2 values are applied to the process, through multiplication with the non-causal T polynomial, following the same receding horizon principle.

The third level has look-ahead capabilities, without model based features. Its action is decisional with a simple logic based on a comparison of the deviation between the modified trajectory and the original one, by defining a certain admissible level of this error. The prediction horizons might be imagined to be the first point of the reference that will be recomputed, situated in the future (noted P_{future} in the table) and the last one (P_{final}) – the end of the toolpath. Its action is on large term, as the modification considers the entire trajectory. The interpolation task should have a very rapid action as the recomputed trajectory is applied from a point situated in the future and meanwhile the error ε grows beyond the imposed limit (as further illustrated in Fig. 7a).

IV. SIMULATION RESULTS

Within the Mikron 740 virtual machining center, simulations below consider the machining of an arc. Two feed drives (X and Y) are in motion, with the same control structure implemented. Each axis has its own reference supervisor, but the decisional level is unique, the reparameterisation of the toolpath being initiated by the first axis for which the error is beyond the imposed limit, set to 0.1mm in order to better see the mechanism acting. The constraints are imposed at 56.6 mm/s on each axis. The diminishing ratio is set to 5% from the initial velocity, fixed at 60mm/s during trajectory generation.

Fig. 5 shows the axial velocities, for the unconstrained and the constrained cases. Changes on the velocity are performed through discontinuous steps, which could lead to additional structural vibrations. Improvements may be achieved considering smooth velocity variations. The effect of the whole predictive structure is obvious in Figs. 6 and 7, where the initial and reparameterised reference trajectories and the corresponding position output are plotted. On the X axis, the zoom Fig. 6b) marks the moment, about 0.15s, when re-generation is started, that is when the error between the modified and the initial trajectory is too large. This is better expressed in Fig. 7a), with the tracking error $x^* - x$.

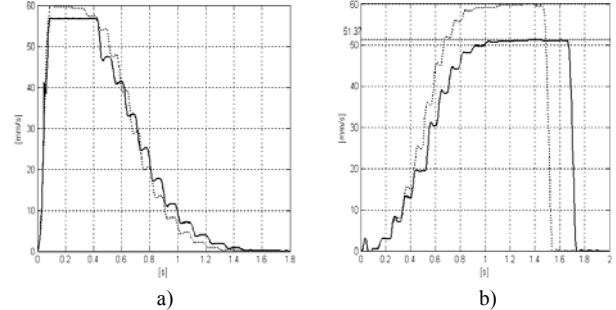


Fig. 5. Axial velocities, unconstrained case – dotted, supervised case – solid. a) X axis; b) Y axis.

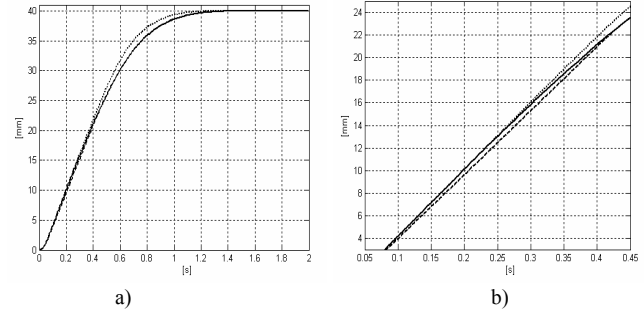


Fig. 6. Reference trajectories: initial – dotted, recomputed – solid, supervised output – dashed. a) X axis; b) Zoom on fig. a).

The constraints are imposed on the two axes, but X comes first to have the velocity setpoint limit reached: the reference supervisor starts to act, modifying the reference; its limits are as well attained, so the decision to reparameterise the whole tool path is taken. Once the regeneration done, the velocities on each axis are both diminished to preserve synchronization, thus at the moment when normally the Y axis supervisor should act (around 0.8s), there is no need as the velocity has already been diminished, reaching 51.37mm/s at the maximum. Thus the tracking error on the Y axis is the same as in the unconstrained case (Fig. 7b).

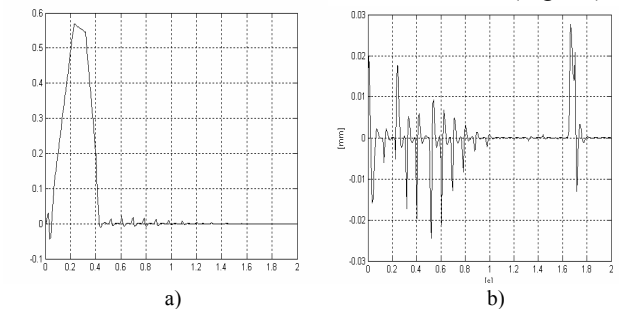


Fig. 7. Tracking errors, supervised case. a) X axis; b) Y axis.

The contour error (Fig. 8b) will be further diminished since the second axis will not add errors, compared to the saturated case where the performances degradation is present on both axes.

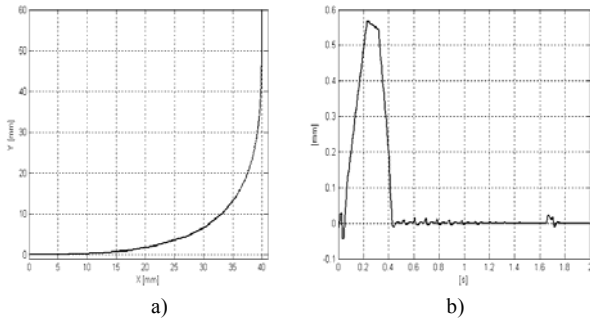


Fig. 8. a) Reference trajectory. b) Contour error.

The corresponding saturated case (realized through GPC implementation with clipping) is presented in the next figures, with the obvious degradation of concerned signals.

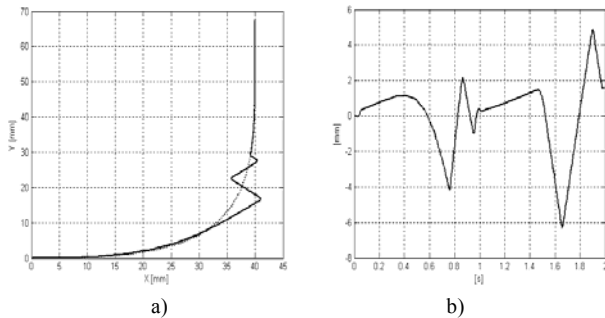


Fig. 9. Saturated case. a) Reference trajectory – dotted, position output – solid. b) Contour error.

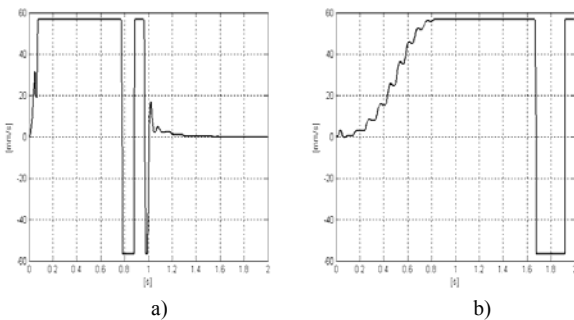


Fig. 10. Saturated case – axial velocities. a) X axis; b) Y axis.

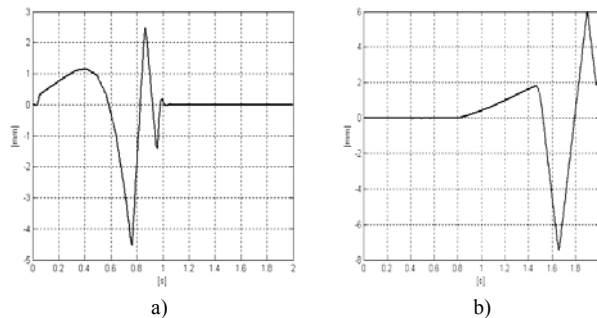


Fig. 11. Saturated case – tracking errors. a) X axis; b) Y axis.

V. CONCLUSION

Implementation of advanced control strategies proved to significantly improve tracking performances, which is of

most importance for axis feed drives in the manufacturing area. The advantages from the advanced knowledge of the trajectory to be followed and the predictive techniques can be used as well for constraints saturation avoidance. The developed mechanism is added to the initial structure without requiring any modification, acting by adapting the reference accordingly. If the constraints are respected, the reference remains unchanged. Within the machining context, manipulating the generation trajectory task, the reparameterisation of the toolpath might be achieved with a diminished velocity is necessary, thus the constraints are avoided with a lower tracking error. The idea is to start with the maximum velocity allowed and to diminish it only if necessary. This way, the contour tracking error is further minimized with the compromise that the machining time will slightly increase.

Concerning the computational aspects, the RST controllers are computed off-line. The RST action is implemented through a simple difference equation. Problems might appear at the trajectory supervisor level, as it proceeds on-line, but again, it might be set on a lower sampling period. For the third option, recomputing the trajectory, this is linked to the capabilities of the reference generation task.

REFERENCES

- [1] Y. Altintas, *Manufacturing Automation – Metal Cutting Mechanics, Machine Tool Vibrations and CNC Design*, Cambridge University Press, USA; 2000.
- [2] Bemporad, A., A. Casavola and E. Mosca, “Nonlinear control of constrained linear systems via predictive reference management”, *IEEE Transactions on automatic control*, Vol. 42, pp 340-349, 1997.
- [3] Boucher, P. and D. Dumur, “Predictive Motion Control”, *Journal of Systems Engineering*, pp. 148-162, 1995.
- [4] A. Casavola, E. Mosca and M. Papini, “Control under constraints: an application of the command governor approach to an inverted pendulum”, *IEEE Transactions on control systems technology*, Vol. 12, pp. 193-204, 2004
- [5] Clarke, D.W., Mohtadi, C. and P.S. Tuffs, “Generalized Predictive Control: Part I The Basic Algorithm, Part II: Extensions and Interpretation”, *Automatica*, 23 (2), pp. 137-160, 1987.
- [6] Erkorkmaz, K. and Y. Altintas, “High speed CNC system design. Part III: High speed tracking and contouring control of feed drives”. *International Journal of Machine Tools & Manufacture*, 41, pp. 1637-1658, 2001.
- [7] Koren Y., *Computer Control of Manufacturing Systems*, International Student Ed; McGraw-Hill, Inc., pp. 143-168, 1983.
- [8] Koren, Y. and C.C. Lo, “Advanced controllers for feed drives”, *Annals of the CIRP*, 41 (2), pp. 689-698, 1992.
- [9] Landau, I.D, *System Identification and Control Design: Using P.I.M. + Software*, Prentice Hall, Inc., 1990.
- [10] G. Pritschow, Y. Altintas, F. Jovane, Y. Koren *et al.*, “Open Controller Architecture – Past, Present and Future”, *Annals of the CIRP*, Vol. 50, pp. 463-470, 2001.
- [11] Rossiter, J. A. *Model-Based Predictive Control. A Practical Approach*, CRC Press LLC, 2003.
- [12] Rodriguez, P., D. Dumur and E. Mendes, “A GPC controller robustification towards measurement noise and parameter uncertainty constraints”, *Proc. ECC*, Cambridge, UK, 2003.
- [13] M. Susanu and D. Dumur, “Advanced axis control implementation within a virtual machine tool environment”, *Proc. IEEE CACSD Conference*, Taipei, pp. 7-12, September 2004.